Mathematical Modeling Anticline Reservoirs

Lourenildo W. B. Leite, Boris P. Sibiryakov and Wildney W. S. Vieira, UFPA, Brazil

This paper was prepared for presentation at the 14th International Congress of the Brazilian Geophysical Society, held in Rio de Janeiro, Brazil, August 3-6, 2015.

Abstract

High and low pressure zones work as natural suction pumps for oil and gas accumulation. In order to localize low pressures zones in sedimentary basins for oil and gas exploration, it is necessary to know P and S wave velocities for the medium. Also, strictly speaking, we need to know the rock densities for all layers, and consider that there are many correlation tables between seismic velocities and densities. Density is a parameter admitted to change slowly with depth, down to the top of the target interface.

This work deals with a theory for stress prediction in the subsurface, and takes in consideration the constitutive parameters (density and Lame's), and the geometry of the reservoir target surface. The model does not separate the different contributions (porosity, fluids) to rock velocities, that is controlled by the constitutive parameters.

Introduction

The anticline structure can be a very useful trap, especially if it has a negative discontinuity in the $\gamma = \frac{V_S}{V_P}$ ratio. In this case, exists also an additional horizontal stretching due to the negative curvature of the anticline structure. It is interesting, that the effects of slope and curvature are in opposite directions; the slopes produce an additional compression, while the average curvature produces a horizontal stretching.

If there is an anticline structure with a positive discontinuity in the γ ratio, it can be a compensational effect. The additional pressure due to the γ discontinuity, and the additional stretching due to the average curvature may eliminate each other. In this case, the anticline structure is not a fluid attractor.

The present work is part of a major project under the theme prediction of stresses and strains using P and S wave velocities in order to localize areas of low pressure in oil and gas productive layers as natural suction pumps. This project is structured in different and independent parts, and as a result the paper Sibiryakov et al. (2013) is published, and others by Sibiryakov et al. (2014a) and Sibiryakov et al. (2014b) have been accepted for publication.

In the present description we restrict our attention to isotropic models. For anisotropic situations the equations are more complicate, there are more control parameters, and the data needs more processing. Every layer forming the 3D geological structural model has constant elastic parameters.

It is mandatory that the acquired data be three components, otherwise it is necessary to apply special processing to obtain the S wave information from P-S phase conversion. S waves can be used from land data obtained with horizontal vibroseis and VSP technology, and from marine data using AVO technology looking for converted P-S-P waves. In special cases, we can use petrophysical measurements of borehole samples for V_P and V_S and density ρ.

The first published appearances about pore space and integral geometry were presented by Sibiryakov (2002) and Sibiryakov and Prilous (2007). The theory of porous media is based on integral geometry, because such mathematical discipline deals with collective geometrical properties of real reservoirs. It has been shown by Santalo (1953) that such collective properties are namely for porosity, specific surface area (SSA), average curvature and Gaussian curvature (Smirnov, 1964). For example, cracked media have as a rule small porosity, but very large specific surface area, what creates anomalous high γ ratio, and it means that the Poisson coefficient, $\sigma = \frac{1-2\gamma^2}{2-2\gamma^2}$, can be negative. This discussion can be seen in Sibiryakov et al. (2013) and Sibiryakov and Sibiryakov (2010).

Methodology

The role of slope angles and curvatures

In order to predict the stress-strain state in geological structures we need to integrate the elastic equations of equilibrium. The boundary conditions are for continuity of forces and displacements. The equilibrium equations contain the elastic parameters; that is, the V_P and V_S velocities, and the rock densities.

These rock parameters and the boundary configuration have to be obtained from the seismic processing and imaging. It means that we need to have detailed velocity analysis from previous investigations. As a special case is the need for the shear wave velocity distribution.

The stresses in geological structures represent a very complicate subject in a six dimensional space, because there are in the usual case six components of the stress tensor in any point of the medium.

The present work analyzes the solution of a simpler problem: the pressure prediction in the vicinity of geologic structural boundaries. The scalar invariant pressure is very important, and it is the simplest characteristic of stress-strain condition. We answer a question about the condition for boundary to be a fluid attractor, or the condition for a boundary not being a fluid attractor.

To give a practical point of view, Figure 1 represents a model for a sedimentary basin, where we aim at a reservoir volume limited on the top by a S surface, where the layers above it are responsible for the overload weight that causes the stress field in the underground rocks. The stress pattern varies according to the γ ratio, that can present important discontinuities across the interfaces. Therefore, the aim is the S surface where the stress discontinuity will varie according to its topographic form, and this effect measured by the spatial slopes and curvatures of the reference S surface. The physical aspects of this theory does not take geological faulting and lithological variations in the rock volume, and only the bending of the formations (above and below the S interface) that defines the anticline structure. For geological representations, special block drawings for reservoir representations are found, for instance, in Chopra and Marfurt (2007).

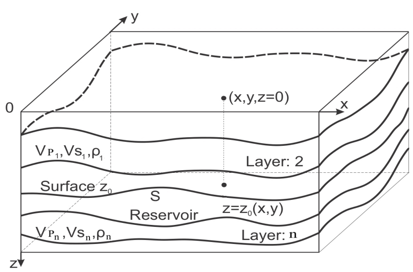

Figure 1: Block perspective illustrating a sedimentary basin. It shows the Cartesian arbitrary system (x, y, z), the layer blocks limited by curved interfaces, a subtle reservoir volume limited above by the S surface represented by $z = z_0(x, y)$, and a flat free surface at $z = 0$.

In the usual case, a geological structure represents a very complicate problem for the solution of the equilibrium equations, which are given by (Novacky, 1975; Kupradze, 1963):

$$\begin{cases} \dfrac{\partial \sigma_{xx}}{\partial x} + \dfrac{\partial \sigma_{yx}}{\partial y} + \dfrac{\partial \sigma_{zx}}{\partial z} = 0 \\ \dfrac{\partial \sigma_{xy}}{\partial x} + \dfrac{\partial \sigma_{yy}}{\partial y} + \dfrac{\partial \sigma_{zy}}{\partial z} = 0 \\ \dfrac{\partial \sigma_{xz}}{\partial x} + \dfrac{\partial \sigma_{yz}}{\partial y} + \dfrac{\partial \sigma_{zz}}{\partial z} = \rho g \end{cases} \tag{1}$$

where the symbology and units are: σ $[N/m^2]$ for stress, ρ $[kg/m^3]$ for density, and g $[m/s^2]$ for gravity acceleration. The spatial variables (x, y, z) stand for the Cartesian system of coordinates, with z pointing positive downwards inside the underground. Physically, the system of equations (1) means that: (1st) the sum of the stress variation along the vertical axis is given by the weight of the overburden column; (2nd) the sum of the stress variation along the horizontal x-axis is chosen to be null; and (3rd) the sum of the stress variation along the y-axis is also chosen to be null. The gravity acceleration, $g = g(z)$, is considered constant in the underground volume in consideration, and also $g = g_z$ when it is needed a convenient notation.

The total solution of the system of equations (1), $u^{(T)} = u^{(C)} + u^{(P)}$, is given by the complementary solution, $u^{(C)}$, of the three homogeneous equations, added to the particular solution, $u^{(P)}$, of the inhomogeneous system obtained via Green's function and convolution (Roach, 1986).

The particular solution for the displacement component $u_k(\mathbf{x}), (k = x, y, z)$, is given by the Poisson integral with respect to the structural volume V as:

$$u_k(\mathbf{x}) = g \frac{1}{V_s^2} \int_V \Gamma_{kz}(\mathbf{x}, \mathbf{y}) dV_{\mathbf{y}}. \tag{2}$$

It is interesting that this integral depends mainly on the shear velocity V_S $[LT^{-1}]$. $\Gamma_{kz}(\mathbf{x}, \mathbf{y})$ $[L^{-1}]$ is the Green tensor for the system of equations (1) (fundamental solution, where in the third equation ρg is replaced by $\rho g \delta(x) \delta(y) \delta(z)$), and it is given by Kupradze (1963).

For the solution represented by equation (2), and others in the sequel based on this formulation (see, for instance, equation (16)), once the displacement field, $u_k(\mathbf{x})$, is known, then the deformation, stress, and pressure fields can be calculated. But, we show ahead for simple models that the contribution of the particular solution in equation (2) is small and, as a result, the complementary solution is more important.

The system of equations (1) with the particular solution in equation (2), and a possible general complementary solution, establish a very complicate problem. To obtain a complementary solution, $u^{(C)}$, is already a special problem by itself.

However, we can obtain an elegant complementary solution to system of equations (1) by considering a plausible model described by simple geometric relations for the S surface, $z = z_0(x, y)$, and by the overburden weight components $P_k = \rho g z n_k$, $[N/m^2]$, in the form:

$$\begin{cases} P_x(S) = \rho g z_0(x, y) n_x \\ P_y(S) = \rho g z_0(x, y) n_y \\ P_z(S) = \rho g z_0(x, y) \end{cases} \tag{3}$$

where $n_i = \cos(n, x_i)$ is the direction cosine between the surface normal vector, $\vec{n}$, and the arbitrary (x, y, z) Cartesian system. The stress expressions for equations (3) (defining σ for normal and τ tangential stress components) on the interface S are written as:

$$\begin{cases} P_x(S) = \sigma_{xx} n_x + \tau_{yx} n_y + \tau_{zx} n_z|_S = \rho g z_0(x, y) n_x \\ P_y(S) = \sigma_{yy} n_y + \tau_{xy} n_x + \tau_{zy} n_z|_S = \rho g z_0(x, y) n_y \\ P_z(S) = \sigma_{zz} n_z + \tau_{xz} n_x + \tau_{yz} n_y|_S = \rho g z_0(x, y) \end{cases} \tag{4}$$

We can now consider that the rock displacements on the boundary $z = z_0(x, y)$ to be related with the vertical displacement by the formulas:

$$\begin{cases} u_x = u_z \cos(\rho g, x) \\ u_y = u_z \cos(\rho g, y) \\ \cos(\rho g, z) = 1 \end{cases} \tag{5}$$

On the boundary, represented by the surface $z = z_0(x, y)$, the vertical strain is given by the relation:

$$e_{zz} = \frac{\partial u_z}{\partial z} = \frac{\rho g z(x, y)}{\lambda + 2\mu}; \tag{6}$$

that comes from equations (1) considering a flat structure. Under integration, equation (6) gives the displacement,

$$u_z(z_0(x,y)) = \int_0^{z_0} \frac{\rho g z(x,y)}{\lambda + 2\mu} dz = \frac{\rho g z_0^2(x,y)}{2(\lambda + 2\mu)}. \quad (7)$$

In the above equation, the quantities ρ and g are allowed to varie as a function of $z(x,y)$; but, the solution in the right hand consider them constant within $z(x,y)$.

The horizontal strain, $e_{xx} = \frac{\partial u_x}{\partial x} = u_{x,x}$, with equation (5), using the convenient symbology, is expressed by:

$$e_{xx} = \frac{\partial}{\partial x} u_z(x,y) \cos(n,x); \quad (8)$$

with the result under derivation by parts,

$$e_{xx} = u_{z,x} \frac{z_{0,x}}{\sqrt{1 + z_{0,x}^2 + z_{0,y}^2}} - u_z \frac{z_{0,xx}}{\sqrt{1 + z_{0,x}^2 + z_{0,y}^2}} \left(1 - \frac{z_{0,x}^2}{1 + z_{0,x}^2 + z_{0,y}^2}\right). \quad (9)$$

For the above equation (9),

$$u_{z,x}(x,y) = \frac{\rho g}{\lambda + 2\mu} z_0(x,y) \frac{\partial z_0(x,y)}{\partial x}. \quad (10)$$

The total dilatation ($\theta = \nabla \cdot \vec{u}$) (vertical compression and horizontal decompression) on the boundary $z = z_0(x,y)$ takes the result:

$$\begin{aligned} \theta(z_0(x,y)) = \;& \frac{g z_0}{V_P^2} \left[1 + \frac{z_{0,x}^2 + z_{0,y}^2}{\sqrt{1 + z_{0,x}^2 + z_{0,y}^2}}\right] \\ & - \frac{g z_0^2}{2V_P^2} \left[z_{0,xx} \varphi_1(x,y) + z_{0,yy} \varphi_2(x,y)\right] \end{aligned} \quad (11)$$

where,

$$\begin{cases} \varphi_1(x,y) = \dfrac{1 + z_{0,y}^2}{\left(1 + z_{0,x}^2 + z_{0,y}^2\right)^{3/2}} \\ \varphi_2(x,y) = \dfrac{1 + z_{0,x}^2}{\left(1 + z_{0,x}^2 + z_{0,y}^2\right)^{3/2}} \end{cases} \quad (12)$$

The quantity named Pressure P is defined as the average of the normal stresses; that is:

$$P = \frac{1}{3}(\sigma_{xx} + \sigma_{yy} + \sigma_{zz}); \quad (13)$$

and it is the first invariant of the stress tensor. Using the generalized Hooke's law for isotropic medium:

$$\sigma_{ij} = \lambda \theta \delta_{ij} + 2\mu e_{ij}; \quad (14)$$

the pressure in equation (13) is now directly related to the dilatation, and we specify it in the form,

$$P_\theta = (\lambda + \frac{2}{3}\mu)\theta = K\theta, \quad (15)$$

where $K = \lambda + \frac{2}{3}\mu$ stands for the pressure module.

Some observations about the dilatation equation (11) are now important.

First, that equation (11) depends on V_P, and on the first and second order space derivatives of the surface $z = z_0(x,y)$. The first derivative terms, $[z_{0,x}(x,y), z_{0,y}(x,y)]$, are slope angles. The second derivative terms, $[z_{0,xx}(x,y), z_{0,yy}(x,y)]$, relate to the surface general curvature (Smirnov, 1964).

Second, in the case that the P wave velocity does not change across the boundary (this is very rare situation), the dilatation has a continuous value. But, in the usual case the P wave has a discontinuity across the boundary and, as given above, the pressure is given by the product of pressure module (K) to the dilatation (θ), that can also change across the boundary (Sibiriakov et al., 2004).

Third, the first term of the equation (11) contains the square of the first derivative, which means that, for not very large angles, the slope effect results in the increase of pressure due to the structure. However, the curvature effect is more interesting.

Fourth, for negative curvature (anticline structure) there is a decrease in pressure, and this effect increases with depth due to the $z_0^2(x,y)$ factor in the second term of equation (11), instead of in the first term where there is the factor $z_0(x,y)$.

Fifth, and continuing, the sign of the second derivative is negative, and the curvature is also of a negative value. This means, the anticline structure produces a low pressure zone, which is a favorable condition for fluid accumulation. For positive curvature (sincline structure), we have the opposite effect.

Sixth, consider the ideal case of a spherical arc; then, the value of the second term in equation (11) may have the value of the first term. This means that the negative curvature produces a planar stretching near the top, and shortening near the rim.

Seventh, the first term in equation (11) is related to the slope angles, with a positive contribution to the dilatation. This means that this term produces an increase in compression as a function of the increase in the amplitude of the anticline structure.

The question that we raise now is: When is it possible that the simple representations in equation (5) is sufficiently accurate to diminish the pressure field in the vicinity of the anticline dome?

It should also be clear that the contributions of the Poisson integral in equation (2) to the displacement and stress fields are small, in comparison to the fields due to elementary geometrical and physical properties of structures (tangent and vertical forces, and displacements along the structure boundary).

Contribution of the Poisson Integral to Displacements

We can represent the contribution of the Poisson integral equation (2) to the displacement field as the difference of two integrals in the form:

$$\Delta u_k(\mathbf{x}) = g\left(\frac{1}{V_S^{(+)2}} - \frac{1}{V_S^{(-)2}}\right) \int_V \Gamma_{kz}(\mathbf{x}, \mathbf{y}) dV_{\mathbf{y}}, \quad (16)$$

where $V_S^{(+)}$ (above) and $V_S^{(-)}$ (below) are seismic wave velocities across the structure S boundary. The integrand is the Green tensor given by:

$$\Gamma_{kz}(\mathbf{x},\mathbf{y}) = \frac{1}{8\pi}\left[(1+\gamma^2)\delta_{kz} + (1-\gamma^2)\frac{(\mathbf{x}_k-\mathbf{y}_k)(z-z')}{r^2(\mathbf{x},\mathbf{y})}\right]\frac{1}{r(\mathbf{x},\mathbf{y})}, \quad (17)$$

where $\mathbf{y} = (x', y', z')$ is the integration variable throughout the volume V. The two integrals in equation (16) are interpreted as material substitution: the first integral relates to the material which is eliminated from the structure, and the second to the material which is occupied by the real structure. Figure 2 illustrates the coordinate system, the geometry of the reservoir volume V, the integration variable $\mathbf{y}$ in the volume V, and the reference point $\mathbf{x}$ along the S surface.

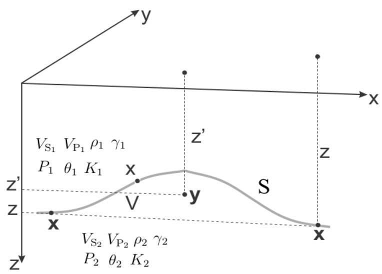

Figure 2: Block diagram representing a reservoir volume V limited above by the surface S represented by $z = z_0(x,y)$. The integration variable $\mathbf{y}$ and the S surface reference point $\mathbf{x}$ are also shown.

The quantity r is the geometrical distance between the $\mathbf{x}$ and $\mathbf{y}$ points. The contribution in equation (16) vanishes if the velocities $V_S^{(+)}$ and $V_S^{(-)}$ are equal. On the other hand, the displacement field due to the elementary method expressed by equations (6) and (7) is given by:

$$u_z^0 = \frac{\rho g z_0^2}{2(\lambda+2\mu)} = \frac{g z_0^2}{2V_P^2}. \quad (18)$$

Let us consider a simple but important structure model represented by a spherical body characterized by the volume $V = \pi R^2 h$, where R is the average radius of the structure, and h is the amplitude. The result for the integral in equation (16) gives a simple and good numerical condition for an estimation method (formulas of the type in equation (11)), that is given by:

$$\frac{Rh}{8}\frac{\Delta V_S}{V_S} \ll 4\gamma^2 z_0^2; \quad (19)$$

where $\Delta V_S = V_S^{(+)} - V_S^{(-)}$. Considering that the γ ratio be about $\gamma^2 \approx 0.25$, then the numerical condition in equation (19) simplifies to:

$$\frac{h}{R}\frac{\Delta V_S}{V_S} \ll 8\left(\frac{z_0}{R}\right)^2. \quad (20)$$

This interesting result says that for small value of h with respect to R, the equation (20) is true, specially for large z_0, and it establishes that a spherical segment represents well an anticline structure.

Results

Figure 3 shows the case of an anticline structure modeled by a Gaussian surface defined by:

$$z_0(x,y) = H - he^{-\left(\frac{x^2+y^2}{a^2}\right)}, \quad (21)$$

where H is the depth to the rim of the structure, a the average radius, and h is the amplitude of the Gaussian dome.

For calculating the pressure across the model surface, the parameters for the two media are defined as: V_P above is 3000 m/s, and 3200 m/s below; $\gamma = V_S/V_P$ above is 0.5, and 0.577 below; the density is $\rho = 3000$ kg/m^3 above and below; and the gravity value was taken as $g = 9.8$ m/s^2. The figures that follow are the results obtained with these parameter values.

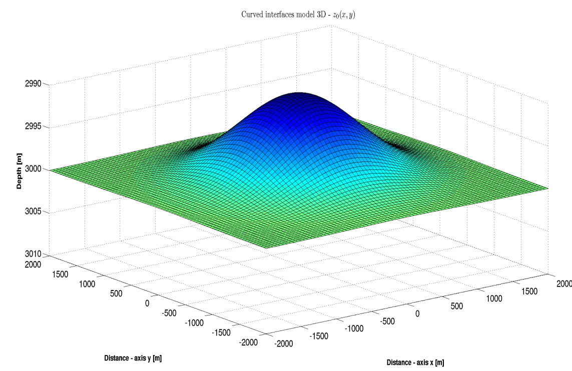

Figure 3: Topography of the anticline model according to equation (21) representing the S surface separating the two media. The vertical axis indicates the surface position and amplitude $z_0(x,y)$ for $h = 10$, $H = 3000$, and $a = 1000$.

Figure 4 shows the elementary overburden pressure field $P_0 = P_z(S) = \rho g z_0$ behavior above the S surface, and with a consistent low around the dome.

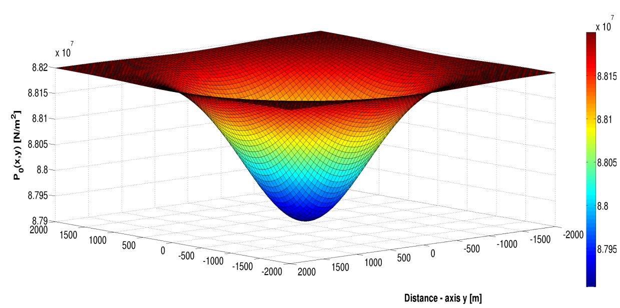

Figure 4: Normal overburden weight as pressure P_0 according to equation (3).

Figure 5 shows the overburden weight pressure discontinuity $\Delta P_0 = \frac{4}{3}P_0(\gamma_1^2 - \gamma_2^2)$ form across the S surface, and with a consistent low around the dome as expected for the given parameters.

Figure 6 shows the cubic dilatation θ calculated with equation (11), where the red color is for the medium above,

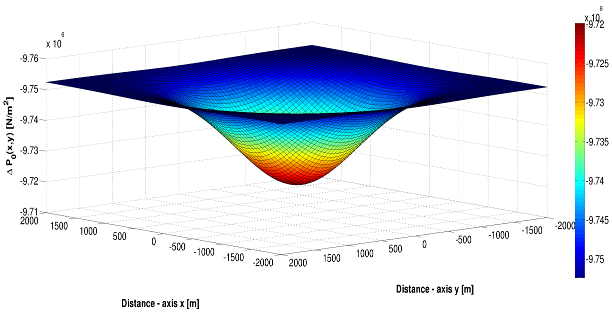

Figure 5: Normal overburden weight as pressure discontinuity ΔP_0 across the S surface, and consistent with the results of Figure 4.

and the green color for the medium below the S surface. The figure shows a consistent form for the dilatation with respect to the specified model.

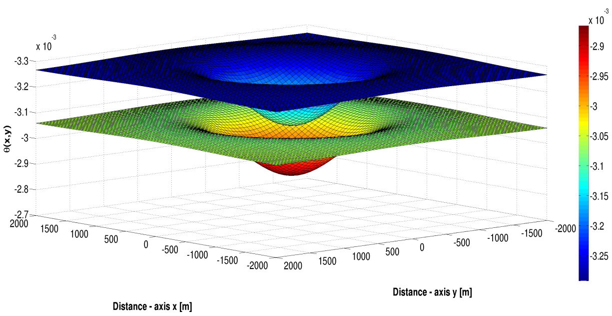

Figure 6: Cubic dilatation θ according to equation (11). The values in green are for the layer below the S surface, and in blue for the layer above S.

Figure 7 shows the distribution of the dilatation pressure P_θ, where is clear a low area around and under the dome. This distribution is calculated by $P_\theta = (\lambda + \frac{2}{3}\mu)\theta = P_\theta(z_0)$ using equation (11) referenced to the S surface $z_0(x,y)$. The pressure immediately above the S surface (blue color) is given by $P_\theta^{(+)} = P_\theta - \frac{1}{2}\Delta P_\theta$, and immediately below (red color) by $P_\theta^{(-)} = P_\theta + \frac{1}{2}\Delta P_\theta$.

The pressure unit used is $N/m^2 = 1$Pascal (Pa), which is equivalent to $1\text{Pa} = 9.8692 \times 10^{-6}$atm (atmosphere).

It is interesting to observe that the pressure below the S surface (blue color) is sufficiently less than the pressure above (red color) by about $1.0 \times 10^7 [N/m^2]$ (about 200 atmospheres). The main role in pressure decrease is played by the negative curvature of the anticline arc, and by the negative discontinuity of the γ parameter. This structure acts as a fluid attractor. Besides, we can see a pressure increase near the periphery of the structure, and this means that around the periphery of an anticline there is a border for fluid migration to below, or to above, the anticline S surface.

Figure 8 shows the pressure discontinuity ΔP_θ across the S surface, where is clear a low pressure area around and under the dome. This is a convenient figure to see the subtlety and details for the analysis of fluid migration around the dome and rim of the structure.

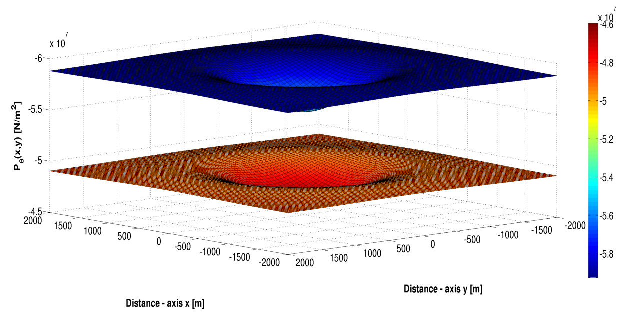

Figure 7: This structure is a fluid attractor. Result for the dilatation pressure P_θ using equation (11) and θ as shown in Figure 6. The blue color is for the medium above, and the red color is for the medium below the S surface.

Fluids should migrate from a high to low pressure zone, but we still have to consider the petroleum geology principles to form a complete analysis of the migration process as, for instance, the source and sealing rocks, and structural attitudes.

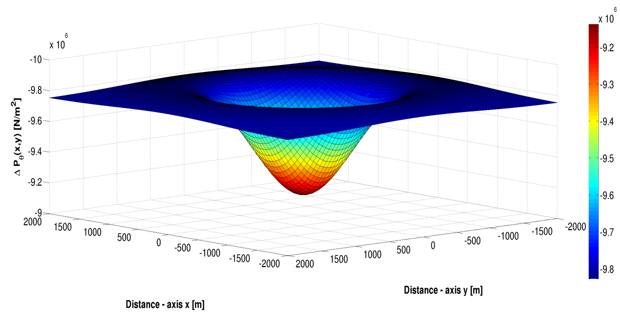

Figure 8: Result for the dilatation pressure discontinuity $\Delta P_\theta = K_1\theta_1 - K_2\theta_2$ using the results in Figure 7 to analyze the details of the pressure variation around the dome and rim.

Figure 9 shows the difference between the pressure discontinuities as calculated by the two related models: overburden minus dilatation pressures, and given by $\Delta P_{0\theta} = \Delta P_0 - \Delta P_\theta$, using results as shown in Figures 5 and 8. The rim area shows the expected value around zero, and the dome presents a discrepancy between these two models, but by only around 0.1 atm, what represents a good approximation considering a discontinuity of 200 atm for ΔP_0 and ΔP_θ.

For the case of Figure 10, we inverted the physical conditions through the parameters of the anticline; that is, $\gamma = 0.577$ above, and $\gamma = 0.5$ below the S surface. The result gives another picture, as the inverse of the Figure 7; that is, the pressure below the S surface is larger than above by about $1.0 \times 10^7 [N/m^2]$ (about 200 atmospheres), and the vicinity of the structure is not a fluid attractor.

Conclusions

Zones of low pressure exist not only in anticline structures; but, they can also be present in horizontal layers if the γ ratio is smaller in the layer above than in the layer below with respect to the structure surface. The search for such zones requires the knowledge of both P and S seismic

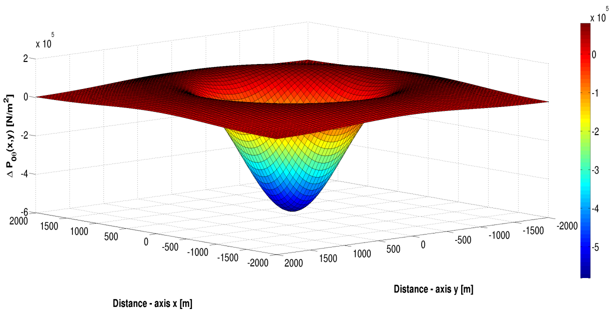

Figure 9: Difference between the overburden and the dilatation pressure discontinuities $\Delta P_{0\theta} = \Delta P_0 - \Delta P_\theta$ using the results as shown in Figures 5 and 8.

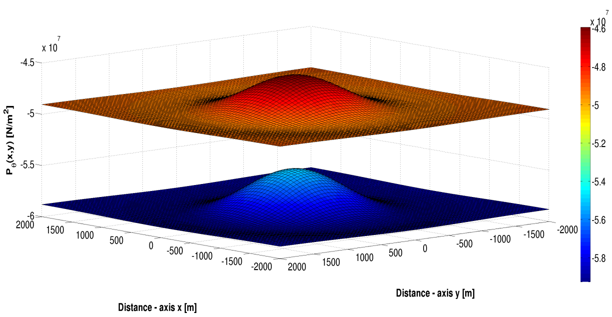

Figure 10: This structure is not a fluid attractor. The parameters have the inverse values of the ones for the case of Figure 7: blue for $\gamma = 0.5$ below, and red for $\gamma = 0.577$ above the S surface.

velocity distributions, which can be determined by seismic processing, VSP and laboratory measurements.

The local decrease of pressure near the dome of an anticline structure depends on the discontinuity of the physical parameters across the structural surface, and on the geometrical parameters (slope angle and curvature). The quantity physically affected is the stress field, and the constitutive parameters (density, Lame's, and if needed the porosity, specific surface area, etc) are admitted constant for the volume rock under the static condition. The volume rocks that form the anticline extend laterally to a horizontal attitude with the same constitutive parameter values.

The negative discontinuity of pressure causes the decrease of pressure below the structure surface, which turns it an attractor for fluid accumulation.

The positive discontinuity of pressure causes an increase of pressure below the structure surface, and as a result this structure is not an attractor feature for fluid accumulation.

The role of structural curvature is to increase its effect on the pressure value as a function of depth of the structure; that means, as the depth increases the role of the curvature also increases.

References

Chopra, S., and Marfurt, K. J., 2007, Seismic attributes for prospect identification and reservoir characterization: Society of Exploration Geophysicists, Tulsa, USA.

Kupradze, V. D., 1963, The potential method in elasticity: Physics and Mathematics Issue, Moscow.

Novacky, V., 1975, Theory of elasticity: Mir, Moscow.

Roach, G. F., 1986, Green's functions: Cambridge University Press, London.

Santalo, L., 1953, Introduction to integral geometry: Hermann and Cia. Editors.

Sibiriakov, B. P., Sibiryakov, E. B., Glebov, A. F., Nesterov, V. N., and Sokolov, E. P., 2004, The prediction of stresses and elements of hydrodynamics by multiwave seismic: Russian Geology and Geophysics, **1**, no. 6, 752–759.

Sibiryakov, B. P., and Prilous, B. I., 2007, The unusual small wave velocities in structural bodies and instability of pore or cracked media by small vibration: WSEAS Transactions on Applied and Theoretical Mechanics Issue 7, **2**, 69–79.

Sibiryakov, E. P., and Sibiryakov, B. P., 2010, The structure of pore space and disjoining pressure in granular medium: Physical Mesomechanics (Special Issue), **13**, 40–43.

Sibiryakov, E. P., Leite, L. W. B., and Vieira, W. W. S., 2013, Model of the structured continuum, and the relation between specific surface area, porosity and permeability: Brazilian Journal of Geophysics, **31**, no. 4, 559–568.

Sibiryakov, E. P., Leite, L. W. B., Sibiryakov, E., and Vieira, W. W. S., 2014a, Local low pressure areas in anticline structures (accepted): Brazilian Journal of Geophysics.

Sibiryakov, E. P., Leite, L. W. B., and Vieira, W. W. S., 2014b, Behavior of stresses and hydrodynamics from multicomponent seismic data (accepted): Brazilian Journal of Geophysics.

Sibiryakov, B. P., 2002, Supersonic and intersonic cracking in rock-like material under remote stresses: Theoretical and Applied Fracture Mechanics, **38**, no. 3, 255–265.

Smirnov, V. I., 1964, Course of higher mathematics:, volume 2 Pergamon Press, London.

Acknowledgments

The authors would like to thank the sponsorship of Project INCT-GP. And in special to the Project Science Without Borders of CNPq/CAPES of the Brazilian Federal Government that has sponsorsed the major part of this research aiming at oil and gas exploration. Also in special to the Project PRH-06 that is present in part of this research. We extend our thanks also to the Project FINEP-Fase-5, and to CAPES for the scholarship.